Improved SPICE Modeling and Analysis of a Thermoelectric Module

Yacouba Moumouni and R. Jacob Baker
Department of Electrical and Computer Engineering, University of Nevada, Las Vegas
yacoubam@unlv.nevada.edu

***Abstract*—An improved SPICE model for a thermoelectric generator (*TEG*) is presented. Temperature variations of the intrinsic internal parameters are included in the proposed model. For accuracy in the proposed model, the internal parasitic components effects and the temperature dependence of the parameters that occur in any thermoelectric module (*TEM*) were taken into account. Experimental results were compiled in the form of a lookup table and then fed into the SPICE simulator using a piecewise linear (*PWL*) model in order to validate the model. Experimental results showed that a differential temperature of 13.43°C was achievable whereas the SPICE model indicated a temperature gap of 9.86°C with the higher error being associated with the hot side. Overall, both experimental and simulated results were in a good agreement.**

***Index Terms*— thermoelectric generator (*TEG*), thermo-electric cooler (*TEC*), Thermo-electrical equivalence, SPICE model, renewable energy, internal parameters.**

I. Introduction

The world population is growing at a much faster rate than ever before. Major sources of energy are in limited supply. Renewable resources on the other hand, are those that are replenished rapidly and naturally. Examples of renewable energy resources include solar, biomass, and geothermal. The thermoelectric module (*TEM*) is considered to be one of the best generators of renewable energy because of their extreme reliability. Furthermore, the TEM has no moving parts. Its main drawback, when compared to other renewable resources, is lower efficiency. As reported in [1] a TEM is only about five to six percent efficient. Even with this low efficiency, the TEM can utilize the abundance of free thermal energy resources for conversion into electrical energy for the benefit of mankind [2]. Thermoelectric solid-state devices directly convert thermal heat into electrical energy or vice-versa. In other words, not only can TEMs be used to convert the energy from the Sun or any kind of wasted heat into electricity, but they also have the potential to transform electrical energy into heating/cooling [3]. How much of the energy is being converted from one form to the other is solely dependent upon the figure-of-merit which is often called "goodness factor" [4].

$$ZT = \alpha^2 \cdot \delta \cdot \frac{T}{K} \tag{1}$$

Where, α, δ, k, and T are the Seebeck coefficient, electrical conductivity, thermal conductivity, and absolute temperature in Kelvin respectively. A key factor to note in Eq. (1) is that the thermal conductivity needs to be lowered for the goodness factor, *ZT*, to be increased and thus the efficiency of the TEM to be improved.

It should be mentioned that TEM technology, as an abundance of literature describes, consists of n- and p-type semiconductors materials connected electrically in series and thermally in parallel. When one side of the TEG is subjected to heat while the other side is at a lower temperature because of a thermal resistance heat exchanger, an electromotive force (ΔV) is generated proportional to the Seebeck coefficient of the TEG semiconductor material as discussed in [5]:

$$V = \alpha \cdot (T_H - T_C) \tag{2}$$

Where T_H and T_C represent the hot and cold side temperatures respectively

On the other hand, if an electrical current flows in the junction, that generates a thermal difference between the two sides of the device; the phenomenon is referred to as the Peltier effect [6]. One side at the junction will absorb heat from while the other side dissipates heat to, the surroundings depending on the amount and the direction of current flow as in Eq. (3).

$$Q = \alpha \cdot T \cdot I \tag{3}$$

Where, I represents the current that flows in the device.

The purpose of this paper is to show both the feasibility of an improved LTspice [7] model for the TEM and, to investigate how laboratory experiments compare to the computer simulations using the developed model. First, the TEM was run as a heat pump or TEC based on both experiments and SPICE simulations. Second, the TEM was simulated as accurately as possible by considering the intrinsic parameters. For this reason, among all the physical phenomena that take place in a TEM, the most dominant mechanisms were given the most attention (i.e., *Seebeck*, *Peltier*, and *Joule effects*). The *Thompson effect* is explicitly neglected in this work due to its smaller contribution in terms of cooling.

The following section briefly describes the test setup for this comparison. Section 3 explains and implements the TEG model in Spice. Finally, Sec. 4 presents, discusses, and compares both experimental and simulated results. This is

followed by a concluding summary of the study's main findings in Sec. 7.

II. The Test Stand Description

For the purpose of this study, one thermoelectric manufacturer's TEM was selected, i.e. Custom Thermoelectric [11]. The particular device's model number is 2411G-7L31-15CX1. Basic specifications for this TEM were supplied by the manufacturer and the other parameters used in the model were extracted in our concurrent work [8]. It is worthy of note to point out that the aforementioned internal parameters, although given as a constant factor, were revealed in [9] to be varying over time. Hence, in order to achieve accurate results, these variations were accounted for in the model presented in this paper.

The module was originally configured to operate as a TEG, but for this specific investigation and to accommodate the current need, it was first run as a Thermoelectric Cooler (*TEC*). For us to be able to achieve that, the polarities of the TEG were reversed in order to constrain it to function as a TEC. The purpose was to create a differential temperature on each side of the device by applying stepped 5 VDC.

The experimental setup is seen in Fig. 1. The experiment included the following items: one TEM, two thermocouples, two aluminum (Al) plates having dimensions of 56mm x 56mm x 12.7mm, one datalogger, one Variable DC power supply, an insulation chamber in order to minimize the effects of the ambient temperature, a laptop, a double way switch (SW), two resistors, and wires. The TEM (2411G-7L31-15CX1) was sandwiched between the Al plates.

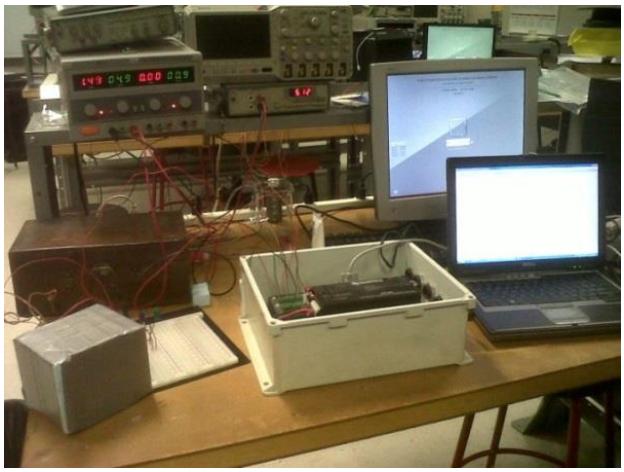

Figure 1 - Experimental setup

Between the Al plates and the two sides of the TEM heat transfer grease was applied. Located each on one side of the module, were the thermocouples for measuring the temperature. These sensors were first engraved into the Al plates via a U-notch groove made by an automatic milling machine. Through the laptop connected to the logger as depicted in Fig. 1, the data were collected and further arranged in a tabular format through the loggerNet software. The 1.7Ω resistor, as seen in the schematic in Fig. 2, served in determining the multiplier (1/*R*) needed to record the current through Ohm's Law. The second, variable, resistor was used for a load. It should be noted at this point that maximum power is transferred only when the internal resistor and the load match. Finally, programming code was written, and transferred, onto the datalogger through the computer. The code is used to facilitate communications between the datalogger and the devices.

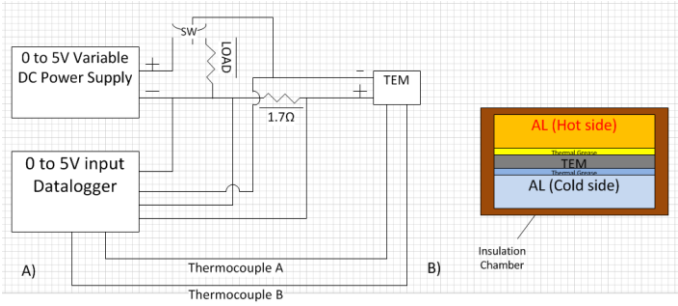

Figure 2 - Block diagram of the setup: a) electrical and b) thermal diagrams.

III. Model Implementation

It is worthy of note that a couple of assumptions were made in order to facilitate the simulations presented in this work. A lookup table of real experimental data was fed into the circuit to improve simulation speed. Hence, due to the complexity in the geometry of the insulation chamber that was used and the corresponding longer time constant, the thermal capacitance value associated with the chamber was neglected. The thermal resistance of the heat transfer grease was assumed to be 0.45*K.W* based on previous studies [7] and [10].

The specific placement of the 23 J/K internal heat capacitance of the TEM was a concern [8]. Either it could be placed on one node or distributed equally between the hot and cold sides. After a few trial simulations, it was clear that the latter yielded better results. The proposed model based on a current-dependent source is presented in Fig. 3. It is an improved version of the circuit presented in [10]. The latter model had the drawback of not utilizing the thermal resistances of the Al plate heat exchangers located on the two sides of the TEM.

The model is implemented using the LTspice software [12] and the work done in [10]. The parameter Seb is the Seebeck coefficient. Likewise, R_{Grease} and C_{Al} are the thermal resistance and thermal capacitance of the thermal grease and Al plates respectively. The thermal resistances of the hot and cold side Al plates are represented by R_8 and R_9. R_{Insul} (*5.9 K/W*) is the thermal resistance of the insulation chamber whereas the internal electrical resistance of the TEM, R_{Int}, is 2.4Ω. R_{Ther} refers to the thermal resistance of the TEM (*here 0.6365 K/W*) as determined from datasheet. The heat capacities of both the ceramic plates and the semiconductor material (Bi_2Te_3) were summed and then equally split into two 12.5 *J/K* capacitances [8]. Each capacitance was then placed on each side of the module. They are represented by C_4 and C_5 as can be seen in Fig. 3.

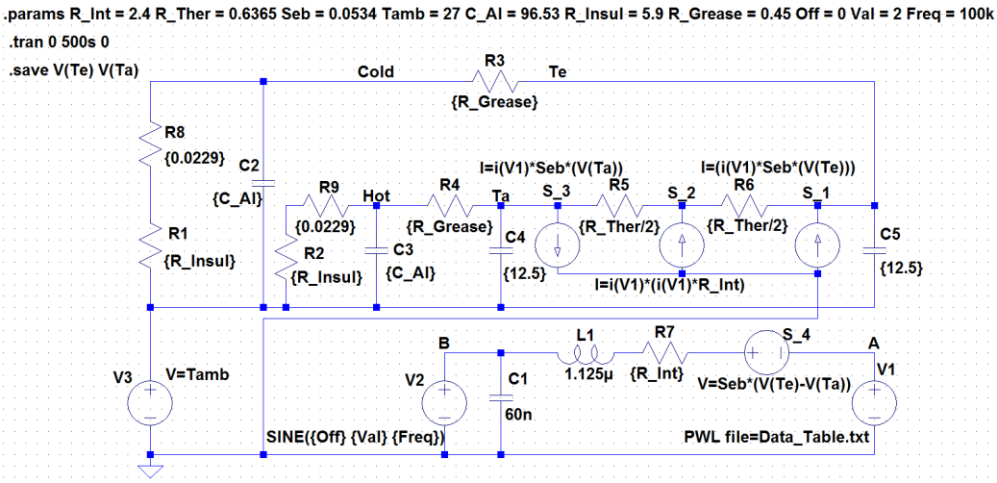

Figure 3 - LTspice model of a TEM with the internal parasitic LC values

The values of the parasitic components C1, and L1 were borrowed from a previous work reported in [10] because they cannot be determined with the equipment available to us.

IV. Results and Analysis

This section presents both the outcomes of the study and a comparison between the experimental results and theory. It is worthy to note that this improved model was run as a TEC under the reverse polarity feature rather that a TEG. Thus, the results of the earlier models (TEG) were expressed in terms of voltage whereas the current model's outcomes are in degrees. Therefore, a direct comparison between the two models is solely excluded in the analysis for simplicity purposes.

The experimental measurements were taken in the period of half an hour. The necessary voltage values used to simulate the real behavior of the heat pump were organized in a table and stored for the simulation in a text file (*labeled "Data_Table.txt" in the simulation schematic seen in Fig. 3*).It is worth mentioning that the length of the simulation was 500 seconds. Longer simulations can take a considerable time to run.

It should also be mentioned that a stepped DC voltage ranging from 1 to 5 V was first applied to the TE device, thus making it work as a heat pump. The purpose of the experiment was to first characterize the device to get familiar with it for future work. After reaching the maximum allowable voltage that the data logger could handle, i.e. 5 V, the supply was kept constant for a while and then cut off.

A significant temperature difference was developed across the two sides of the TEM as can be seen in Fig. 4. The maximum differential value attained within that short period of time was 13.43°*C*. Hence, as expected, the TE device performed as a heat removal device, that is, it performed as a TEC.

During the course of this study, it was clearly observed that the hot and cold sides were departing from one another with the former absorbing heat and the latter releasing it as can be seen from Fig. 4. This fact holds for not only the period whereby the applied voltage was increasing, but also for the whole period it stayed constant at 5 V as stated above.

Simulation results expressed temperatures as voltages, Fig. 5. Also, as already stated above, the simulation time was shorter than the actual time. Figure 6 compares the simulated results against the simulated results. The overall percent error between the experiment and the simulation was 5.47% on the hot side as compared to 2.52% on the cold side.

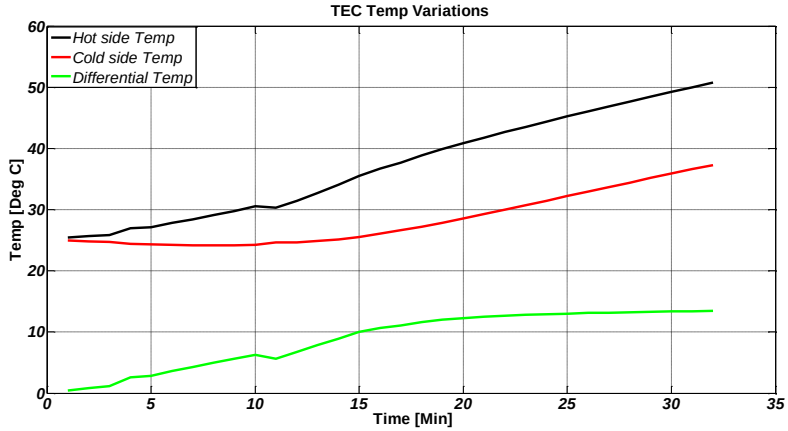

Figure 4 - Experimental temp profile on both sides.

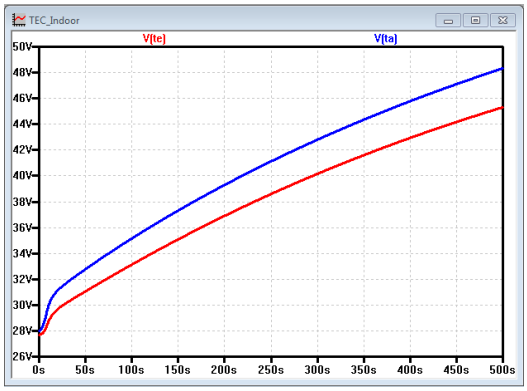

Figure 5 - Simulated temperature profiles, V(ta) represents the hot side and V(te) represents the cold side.

The error rate can be explained by either one or both of the followings: 1) the internal parasitic components' variation and, 2) the non-homogeneity of the physical blocks that were assumed to be pure metals during the thermal and/or electrical parameters computations [8].

V. CONCLUSION

An experimental setup was designed and built to characterize and study the performance of a commercial TEM. An LTspice TEM modeling scheme was developed through thermal to electrical equivalence strategies. The module, though manufactured to be operated as a TEG, was run in this setup as a TEC under the technique of the reverse polarity features. The experiment was conducted for a short period of time (32 minutes) with a variable input supply voltage starting at 0.8V. The source was incremented by 0.5 VDC every minute until the maximum limit of 5 V DC was reached. At the end of the experiment the data were arranged in a lookup table and fed into the SPICE model through the PWL option. Despite the test being conducted for a short period of time a differential temperature of 13.43°C was attained. Finally, the paper experimental and simulated results were presented and compared.

REFERENCES

[1] D. M. Rowe, "Thermoelectric harvesting of low temperature natural/waste heat," *AIP Conf. Proc.*, vol. 485, pp. 485–492, 2012.

[2] D. M. Rowe, "Thermoelectrics, An Environmentally-Friendly Electrical Power," *Renew. Energy*, vol. 16, pp. 1251–1256, 2008.

[3] K.-H. Wu and C.-I. Hung, "Effect of substrate on the spatial resolution of Seebeck coefficient measured on thermoelectric films," *Int. J. Therm. Sci.*, vol. 49, no. 12, pp. 2299–2308, Dec. 2010.

[4] R. McCarty, "Thermoelectric Power Generator Design for Maximum Power: It's All About ZT," *J. Electron. Mater.*, vol. 42, no. 7, pp. 1504–1508, Oct. 2012.

[5] M. G. Molina, L. E. Juanicó, and G. F. Rinalde, "Design of innovative power conditioning system for the grid integration of thermoelectric generators," *Int. J. Hydrogen Energy*, vol. 37, no. 13, pp. 10057–10063, Jul. 2012.

[6] C. Alaoui, "Peltier thermoelectric modules modeling and evaluation," *Int. J. Eng.*, no. 5, pp. 114–121, 2011.

[7] S. Lineykin and S. Ben-yaakov, "Modeling and Analysis of Thermoelectric Modules," *IEEE Trans. Ind. Electron.*, pp. 2019–2023, 2005.

[8] Y. Moumouni and R. J. Baker, "Concise Thermal to Electrical Paramters Extraction of Thermoeleectric Generator for Spice Modeling," submitted for publication in MWSCAS 2015.

[9] M. Cernaianu and A. Cernaianu, "Thermo electrical generator improved model," *Int. Conf. Power ...*, vol. 13, pp. 343–348, 2012.

[10] A. Gontean and M. O. Cernaianu, "Parasitic elements modelling in thermoelectric modules," *IET Circuits, Devices Syst.*, vol. 7, no. 4, pp. 177–184, Jul. 2013.

[11] http://www.customthermoelectric.com/MaterialProperties.htm, accessed July 29, 2014.

[12] http://www.linear.com, accessed July 31, 2014.

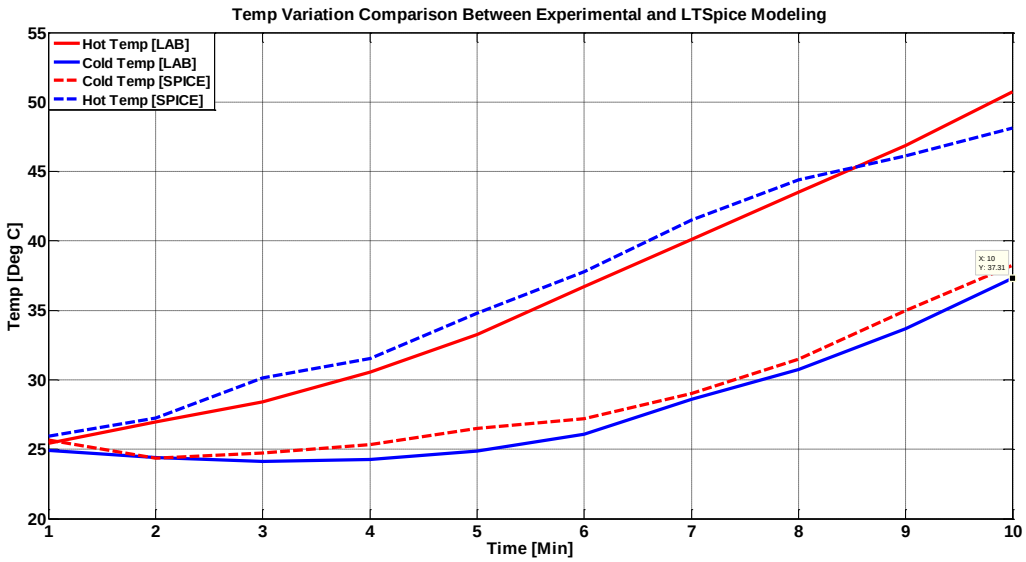

Figure 6 - Temperature profiles, simulated (dashed) and experimental curves (solid).